Analysis of Membrane Support Structures for Integrated Antenna Usage on Two-Dimensional Photonic-Bandgap Structures

Andrew L. Reynolds, Harold M. H. Chong, Iain G. Thayne, John M. Arnold, and Peter de Maagt, *Member, IEEE*

***Abstract*—The study of the transmission of electromagnetic waves through a photonic crystal with various membranes placed over the surface is presented in this paper. A difference in performance is observed even for a membrane thickness that is unable to support guided substrate modes through total internal reflection. The transmittance has been investigated for two crystal orientations, assuming normally incident external plane waves on a finite thickness two-dimensional (2-D) photonic crystals both with and without a membrane. The angular transmission response is characterized by scanning the incidence angle of the impinging plane wave to cover all available angles within the 2-D periodic plane of the structure.**

***Index Terms*—Antennas, electromagnetic crystals, periodic structures, photonic bandgap crystals.**

I. Introduction

SINCE their discovery and first demonstration in the late 1980's, interest in photonic crystals has grown explosively. Looking at literature, it is clear that the emphasis is placed more and more on applications and detailed modeling instead of demonstrating feasibility. One of the applications for photonic crystals is in the field of (sub)millimeter-wave antennas.

A new generation of scientific space-borne instruments has been projected, the frequency range of which may even extend above 3 THz.

As the frequency increases, a planar structure that integrates the antenna, mixer, local oscillator, and all peripheral circuitry onto one single substrate becomes an attractive option.

While conceptually simple, in practice, it is challenging to develop and test an integrated planar antenna on a semiconductor substrate (high dielectric constant) that has good radiation efficiency and can be easily integrated with the active circuit. One of the problems that has been encountered is the fact that planar antennas on dielectric substrates couple power into substrate modes and, since these do not contribute to the primary radiation pattern, substrate mode coupling is generally considered as a loss mechanism.

It is exactly to overcome this where a photonic bandgap (PBG) crystal can find its application. There are several methods for accurately analyzing the electromagnetic properties of PBG crystals. Photonic crystals have received considerable attention during the last decade with the realization that they can control the electromagnetic radiation by forbidding propagation. Pioneering work by both Yablonovitch [1] and John [2] in the late 1980's demonstrated this property in periodic microwave structures. These same principles are now being applied even at optical frequencies. The theoretical models that are most commonly used range from those that calculate the band structure and mode patterns within a photonic crystal as obtained using the plane-wave method [3] and Green's functions [4], [5] to derivation of the reflection and transmission coefficients from the transfer matrix method (TMM) [6], [7]. Excellent agreement with experiments has been achieved with these methods, reinforcing the role that theoretical analysis can play in the design and pre-experimental phases. As most analysis methods assume infinitely sized crystals, caution must still be exercised. However, the TMM allows the transmission and reflection coefficients to be obtained for a finite thickness photonic crystals.

Photonic crystals often have large air spaces between the periodic elements that cannot provide support for the suspension of the metallic elements of either a radiating element, connecting transmission line, or other parts of an antenna system. The fabrication of an antenna system, including the mixer, local oscillator, and all other peripheral circuitry onto a thin low-loss dielectric membrane allows continued repositioning of the antenna on a PBG substrate to further investigate the antenna performance as a function of both position and orientation [8], [9]. As such, the membrane provides a versatile resource in the system. However, as the operational frequency of the system increases, fabrication issues regarding accuracy and the resolution

Manuscript received June 8, 2000. This work was supported by the European Space Research and Technology Center under Contract SRON STS-KJW-96/067. The work of A. Reynolds was supported under an Engineering and Physical Sciences Research Council Studentship Award.

A. L. Reynolds was with the Electromagnetics Division, European Space Research and Technology Centre, 2200 AG Noordwijk, The Netherlands. He is now with Nortel Networks UK Ltd., Harlow, Essex CM 17 9NA, U.K.

H. M. H. Chong, I. G. Thayne, and J. M. Arnold are with the Photonic Band Gap Materials Research Group, Department of Electronics and Electrical Engineering, University of Glasgow, Glasgow G12 8LT, Scotland.

P. de Maagt is with the Electromagnetics Division, European Space Research and Technology Centre, 2200 AG Noordwijk, The Netherlands.

Publisher Item Identifier S 0018-9480(01)05053-0.

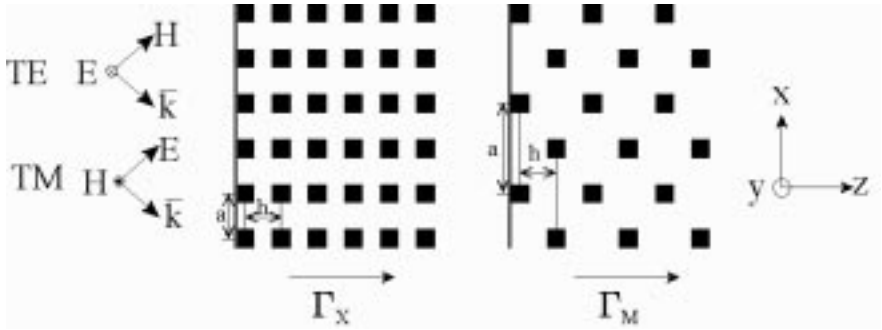

Fig. 1. 2-D crystal orientation, Where a is the periodic spacing of the bars in the x-direction, h is the mid point–point separation of the bars in the z-direction. The membranes have been applied only to the first layer of bars in both lattice configurations.

of manufacture, while maintaining rigidity, set a limit regarding the minimum thickness of the membrane. Thus, although theoretically such systems scale perfectly with frequency, it is beneficial to prototype such systems at the highest frequency possible and limit the scaling factor to orders of a few.

In this paper, the TMM is used to theoretically investigate the effect of placing membranes on the surface of finite-thickness two-dimensional (2-D) periodic photonic crystals, and experimental data at millimeter-wave frequencies is presented to verify the findings.

II. TMM

The TMM as described by Bell *et al.* [6] and Pendry [7] for analyzing the reflection and transmission characteristics of stacks of layers that are 2-D periodic in the plane of the layers has been implemented. The transfer matrix relates the electric and magnetic fields between the two interfaces of this stack in the third finite dimension, which can be used to formulate a scattering matrix. Subsequent cascading of the scattering matrices for each layer allows the transmission and reflection coefficients to be calculated. Dissimilar scattering matrices are included into the transfer matrix routines, as outlined in [6], allowing us to easily add the membrane onto the surface of the PBG crystal. The boundary condition that no inward propagating wave exists in the half-space beyond the stack not illuminated by the illuminating plane wave is applied. This is sufficient to determine the transmission coefficient of the plane wave, which exits from the stack propagating parallel to the incident plane-wave direction, along with the amplitude and phase of all the associated diffraction orders.

III. Lattice Definitions

The influence of two membrane materials (silicon and kapton, i.e., $\varepsilon_r = 11.7$ and $\varepsilon_r = 3.7$, respectively) is examined as a function of membrane thickness. The membrane is placed over the illuminated surface of a 2-D PBG crystal consisting of dielectric bars of silicon. Fig. 1 shows the 2-D lattice configurations used, the normal incidence condition defining the crystal orientation ΓX and ΓM [10]. A general ΓM lattice with every second row displaced by a fractional part of the lattice constant a can be interleaved [10] to form the layer by layer or woodpile crystal [11]–[15]. Our structure interleaves to form the woodpile as suggested by Ozbay *et al.* in [12], which possess a full three-dimensional (3-D) PBG. The 2-D PBG crystals studied in this paper have $a = 1275$ μm and $h = 780$ μm, the silicon bars have dimensions 340×390 μm in the x- and z-directions, respectively. Finally, the definition of TE (TM) polarized waves is noted as those which have their H-field (E-field) confined to the xz-plane, that is to say, the E-field (H-field) parallel to the y-axis (see Fig. 1).

IV. Membranes in Isolation

The application of a membrane on the top surface of a PBG crystal may lead, through external excitation, to substrate modes within the membrane. The cutoff frequencies for substrate modes within a membrane, without considering the PBG crystal, are well known and are described by the following [16]:

$$f_c = \frac{nc}{2h\sqrt{\varepsilon - 1}} \tag{1}$$

where f_c is the cutoff frequency of the mode, c is the speed of light in vacuum, n is the order of the mode, h is the thickness of the membrane, and ε is the dielectric constant of the waveguide constituent material.

Given the intended operation frequency of the system, precautions can be taken to ensure that the membrane will not support any totally internally reflected (TIR) waves giving rise to guided modes within the membrane.

While there is no real angle that will allow a substrate or guided mode to be excited within an isolated membrane from an air medium, when the membrane is placed upon a PBG crystal, it may form a grating coupler. Grating couplers can be thought of as effective waveguides with an effective dielectric constant and thickness. The dielectric constant lies between the values of embedding medium and the larger dielectric constant of its constituent materials, i.e., air, dielectric bars, and membrane. Guided waves can be excited as the wave vector within the effective guide is larger than for air allowing the first-order diffraction orders (excited in the transverse direction to the normally incident plane wave, the yx-direction in Fig. 1) to exist before the onset of conventional diffraction. As the PBG region for the crystals is in the range of 90–100 GHz, a silicon membrane thickness in excess of some 458 μm would be required to support the TM_1 guided mode at 100 GHz. A grating coupler consisting of a single layer of bars with dimension of 390 μm and a membrane with thickness of 100 μm, totaling 490 μm, will re-

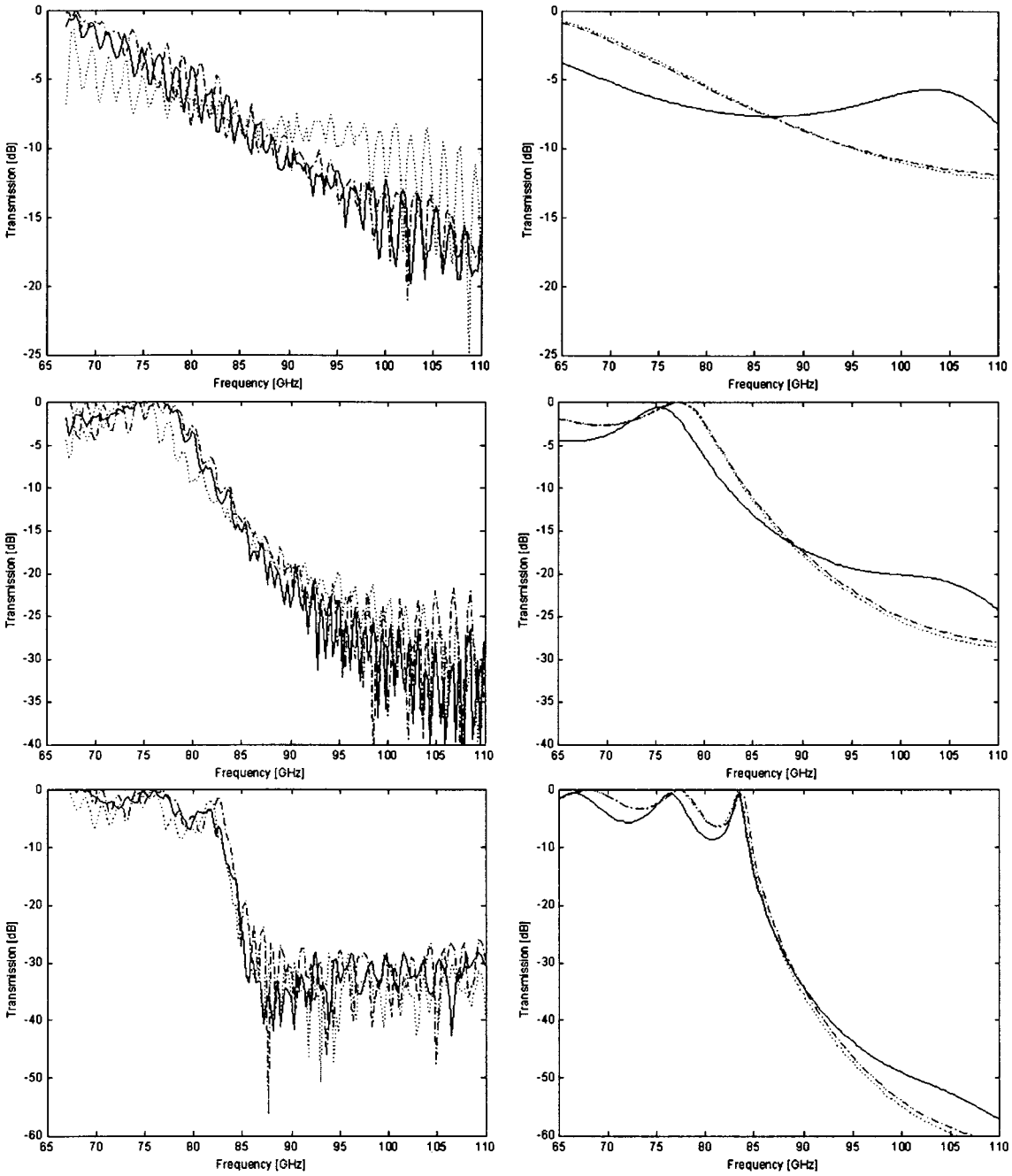

Fig. 2. Gamma-X lattice: measured and theoretical TM response. Top, middle, and bottom plots correspond to the TM transmission response for a crystal thickness' $L = 2h, 4h$, and $8h$ thick. Plots on the left, dashed–dotted, dotted, and solid lines correspond to the no-membrane case, 25-μm kapton membrane and 100-μm silicon membrane, respectively. Plots on the right, dashed–dotted, dotted, and solid correspond to the theoretical response for the no-membrane case, 25-μm kapton membrane, and 100-μm silicon membrane, respectively.

sult in an "effective waveguide." As the effective dielectric constant will be less than that of silicon and the effective width of the guide will be less than 490 μm, the initial layer of bars and membrane will, therefore, not support a parasitic guided mode at 100 GHz.

V. Membranes on a Photonic Crystal—Normal Incidence

Theoretical and experimental analysis of the 2-D crystals with and without membranes has been carried out from 67 to 110 GHz, defined by the range of operation of the vector network analyzer (VNA) used in the experiments. A 100-μm silicon membrane and 25-μm kapton sheet were independently analyzed on the surface of both the ΓX- and ΓM-oriented 2-D lattices for varying thickness of the underlying PBG crystal. Full two-port S-parameters of the structures were measured in the 67–110-GHz frequency range using an Anritsu 360B VNA. The VNA has short WR-10 waveguide sections at the test ports to which standard gain horns were connected. The horn separation was around 80 mm, with the membrane/PBG structure between.

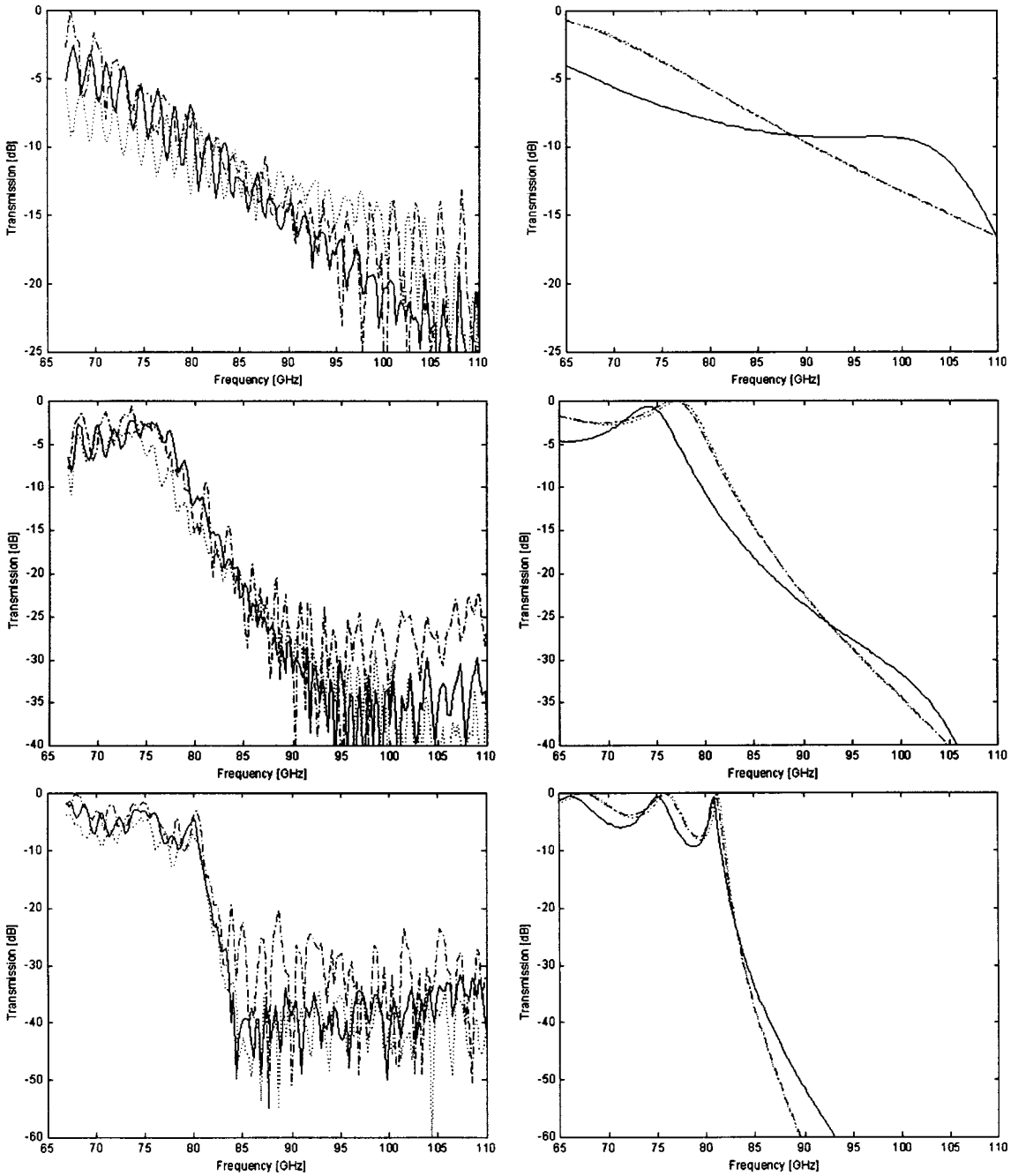

Fig. 3. Gamma-M lattice: measured and theoretical TM response. Top, middle, and bottom plots correspond to the TM transmission response for a crystal thickness' $L = 2h, 4h$, and $8h$ thick. Plots on the left, dashed–doted, dotted, and solid correspond to the no-membrane case, 25-μm kapton membrane, and 100-μm silicon membrane, respectively. Plots on the right, dashed–dotted, dotted, and solid correspond to the theoretical response for the no-membrane case, 25-μm kapton membrane, and 100-μm silicon membrane, respectively.

The measurement system was calibrated using the line–reflect–line (LRL) method using a Flann Microwave bronze WR-10 waveguide calibration kit, which comprises a quarter-wavelength offset, fixed termination, flush short circuit, and through waveguide section. After calibration, the measurement reference planes are situated at the flanges of the short sections of waveguide at the test ports of the VNA to which the standard gain horns were subsequently attached. Thus, 0-dB transmission loss refers to the situation when the short lengths of waveguide at the VNA test ports are joined. A small additional loss and uncertainty will be introduced by attaching the horns after calibration, but this will be relatively small compared with the internal VNA system losses whose influence is removed by this calibration procedure.

Fig. 2 shows good agreement between the theoretical predictions and measurements made on the ΓX-oriented lattice. As the crystal thickness is increased, we see a steady increase in the attenuation of the transmitted normally incident plane wave through the structure. For increasing crystal thickness L, we observe the gradual formation of the lower band edge, expected at 84 GHz and measured at 82.5 GHz for a crystal $L = 8h$, i.e., eight periods thick. Measurements were limited by the $-$35-dB

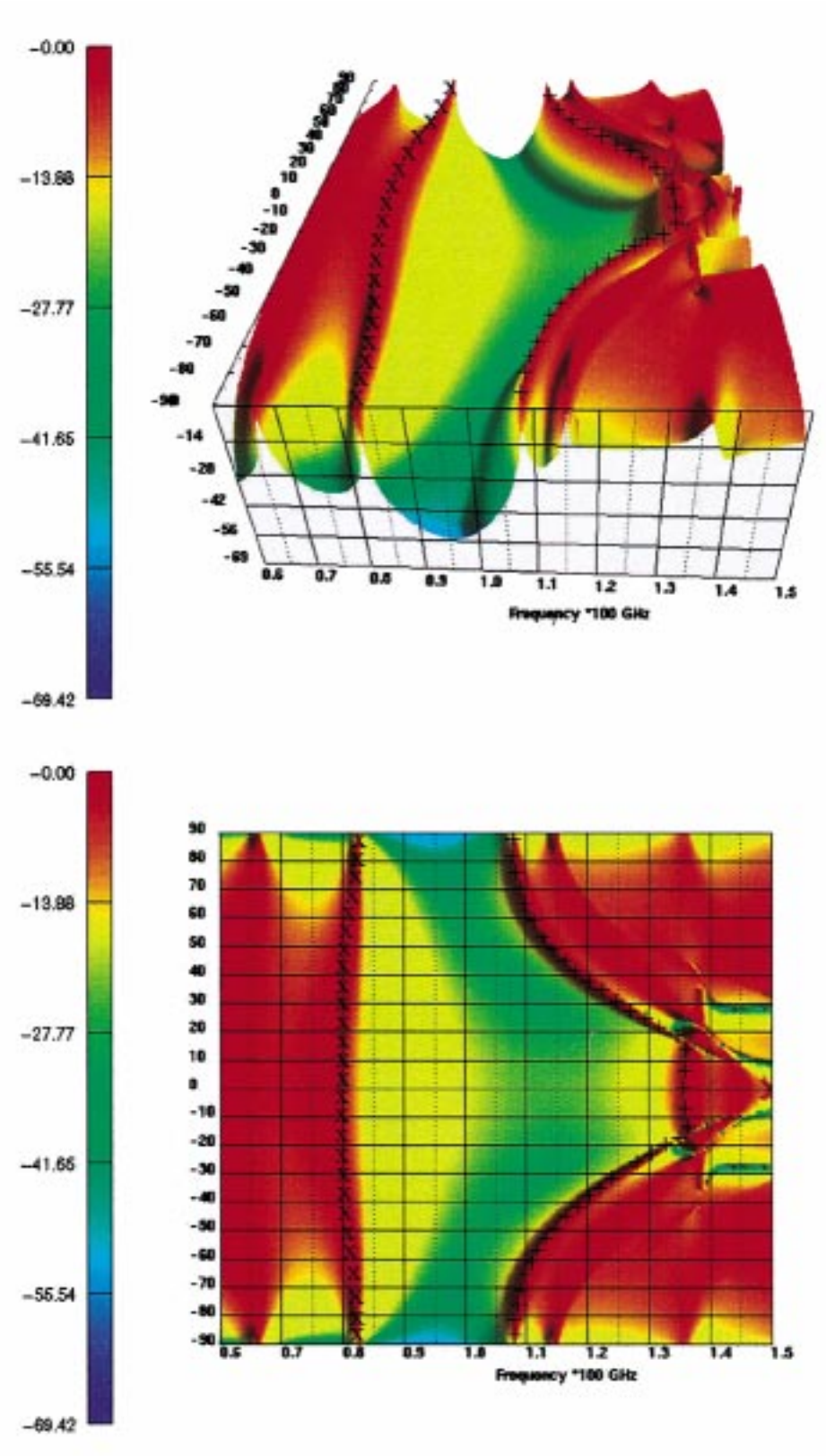

Fig. 4. Perfect crystal angular transmission response. The response is shown for a crystal four periods thick in the z-direction. The crystal is made from silicon bars, 340 $\times$ 390 μm, with a period of 1275 $\times$ 780 μm in the x- and z-directions, respectively. The upper and lower band edge envelopes have been highlighted with "$+$" and "$\times$" symbols to guide the eye. The information displayed in the two plots is the same, but shown from a different perspective.

noise floor of the measurement setup. The influence of the membrane is more prominent for the thinner PBG crystals with the 100-μm silicon membrane than for the thicker crystals. Transmission through the $L = 2h$ crystal is decreased with a 100-μm silicon membrane in the 65–85-GHz region before increasing the transmission response over the 85–110-GHz region. The ΓX

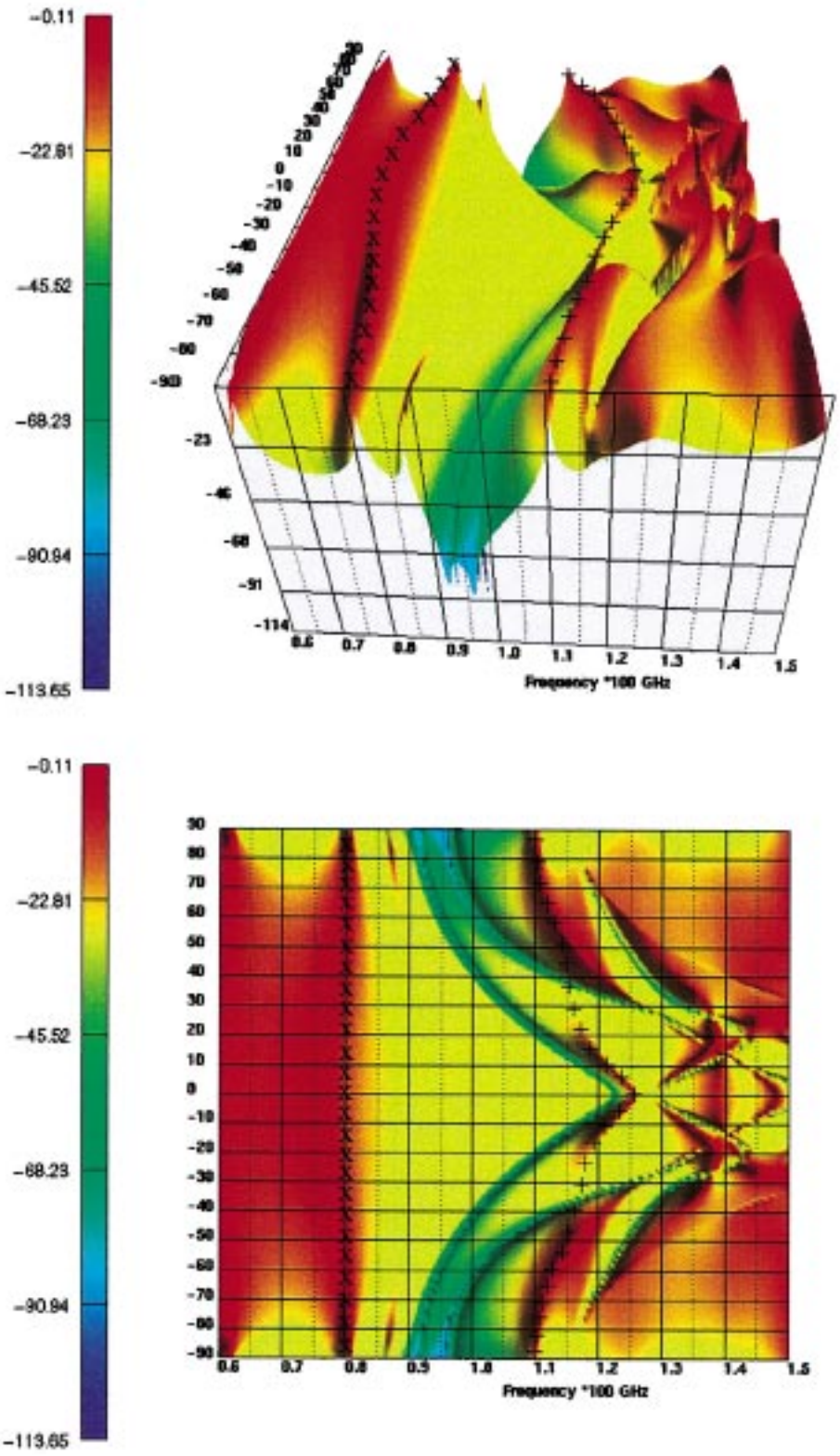

Fig. 5. 100-μm silicon membrane response on the otherwise perfect crystal. The response is shown for a crystal four periods thick in the z-direction. The crystal is made from silicon bars, 340 $\times$ 390 μm, with a period of 1275 $\times$ 780 μm in the x- and z-directions, respectively. The upper and lower band edge envelopes have been highlighted with "+" and "$\times$" symbols to guide the eye. The information displayed in the two plots is the same, but shown from a different perspective.

kapton membrane has little effect on the response for all crystal thicknesses. The 100-μm silicon membrane slightly down shifts the lower band edge for all crystal thickness for the ΓX-oriented lattice, out with the measurable range for the $L = 2h$ lattice, from 78 to 76 GHz for the $L = 4h$ lattice and from 82.5 to 81.5 GHz for the $L = 8h$ lattice. These values are in excellent

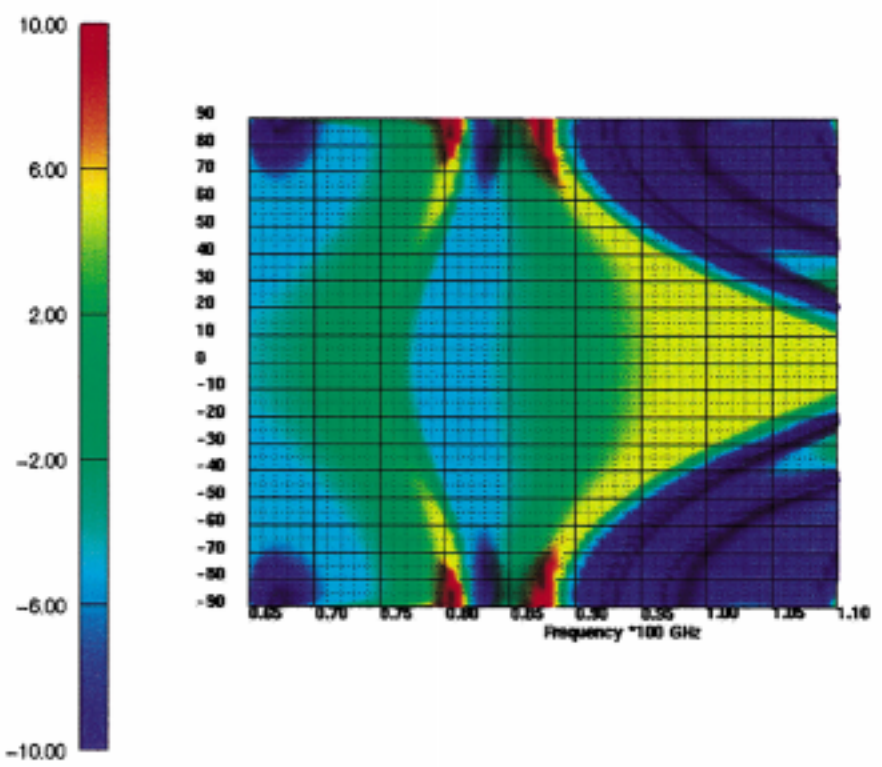

Fig. 6. Difference in the TM transmission. The difference in response is shown between the no-membrane case and 100-μm silicon case for a crystal four periods thick in the z-direction. The crystal is made from silicon bars, 340 $\times$ 390 μm, with a period of 1275 $\times$ 780 μm in the x- and z-directions, respectively.

agreement with the theoretical predictions. As the underlying PBG substrate thickens, the perturbing influence of the membrane weakens, demonstrating that, as the crystal thickens, the PBG behavior is more dominant.

Similar trends are observed with the ΓM lattice, as shown in Fig. 3. The 25-μm kapton membrane has little effect on the transmission measurements relative to the PBG crystal without a membrane present. The 100-μm silicon membrane again shifts the lower band edge frequency, but shows convergent behavior with the nonmembrane case as the crystal thickens, as was observed for the ΓX-oriented crystal. From the theoretical calculations, the attenuation for the ΓM lattice per layer thickness is nearly twice as large as that of the ΓX-oriented crystal, although the experimental noise floor of the system prevented experimental verification for the thicker crystals. Membranes have the interesting effect of enhancing the lower band edge gradient of cutoff, an effect most noticeable for both the kapton and silicon membranes for the $L = 8h$ ΓM-oriented crystal. This is echoed in the measurements, which show the kapton and silicon response curves attaining transmission levels in the noise floor before the crystal with no membrane.

VI. Membranes on a Photonic Crystal—Angular Response

The angular transmission response is characterized by scanning the incidence angle of the impinging plane wave to cover all available angles within the 2-D periodic plane of the structure. From Fig. 4, it can be seen that the normal incidence condition, angle $= 0^\circ$ sets the upper frequency limit of the lower band edge, while the lower frequency edge of the upper band is found close to oblique incidence. The total bandgap lies between 84–108 GHz. Fig. 5 shows the angular response of four periods of the crystal with a 100-μm silicon membrane placed over the front surface. It is obvious that this markedly alters the response of the structure.

Comparing Figs. 4 with 5, there are evident differences. For angles close to normal incidence, the upper band edge has dropped from 130 to 120 GHz. There is also considerable alteration in the higher frequency region with the effect that the upper band envelope has been smoothed when compared to the perfect crystal case. It is noteworthy that the lowest frequency limit of the upper band edge is located at a slightly higher frequency, i.e., 110 GHz, when compared to the perfect crystal response of 108 GHz.

However, the upper frequency limit of the lower band edge, still defined by the normal incidence condition at 0°, is now less well defined and has marginally moved downwards in frequency.

Fig. 6 shows the difference in the TM polarization transmitted level between the perfect crystal lattice and the same lattice with the 100-μm silicon membrane included. The plot has been limited only to show a 10-dB deviation, areas, which have a deviation larger than 10 dB, shown in white. Limiting the discussion to the complete TM bandgap region, between 85–110 GHz, the main concern is the possible existence of surface waves that may exist within the membrane in conjunction with the top layer(s) of bars. Such waves are noted by a characteristic extreme drop in transmission or peak in reflection. These effects are not seen for the range of frequencies studied for the silicon membrane and underlying bars implemented.

For the other regions with large deviations in transmission within the bandgap, (the regions at 80.5 and 82.5 GHz are within the lower band edge), the deviation assists the bandgap behavior as it reduces the transmitted level through the crystal. There is a small region that increases the transmitted level through the crystal at 87.5 GHz, but when the same region is examined in Fig. 5, the total transmitted level is not above -25 dB.

VII. Conclusion

We have shown that the application of a membrane onto the surface of a 2-D photonic crystal, while interacting with the underlying crystal, does not seriously perturb the transmission response of a thick PBG substrate, displaying that the PBG behavior is more dominant. For the regions that we have studied, the application of a membrane actually has helped to steepen the gradient of the lower band edge cutoff frequency aiding the PBG performance of the crystal. However, the upper frequency limit of the experimental setup did not allow measurement of the effect of the membrane on the upper band edge of the crystal. The membranes studied, i.e., 100-μm silicon and 25-μm kapton, are unable to support TIR guided modes at the frequency of the PBG. Theoretical and experimental work has demonstrated that these membranes are good candidates as substrates onto which an antenna system can be fabricated before integration onto the surface of a photonic crystal. This will allow further investigation into the optimal orientation, radiation pattern, and efficiency of integrated antenna systems in the millimeter, submillimeter, and near infrared wavelength ranges.

Acknowledgment

The authors would like to thank Dr. A. Ward, Imperial College London, London, U.K., and Dr. U. Peschel, Friedrich-Schiller-Universitat, Jena, Germany, for their helpful discussions.

References

[1] E. Yablonovitch, "Inhibited spontaneous emission in solid state physics and electronics," *Phys. Rev. Lett.*, vol. 58, p. 2059, 1987.
[2] S. John and N. M. , "Strong localisation of photons in certain disordered dielectric super lattices," *Phys. Rev. Lett.*, vol. 58, p. 2486, 1987.
[3] G. Kweon and N. M. Lawandy, "Quantum electrodynamics in photonic crystals," *Opt. Commun.*, vol. 15, no. 3–4, pp. 388–411, July 1995.
[4] A. J. Ward and J. B. Pendry, "Calculating photonic Green's functions using a nonorthogonal finite difference time domain method," *Phys. Rev. B, Condens. Matter*, vol. 58, no. 11, pp. 7252–7259, 1998.
[5] Y. D. Yang, N. G. Alexopoulos, and E. Yablonovitch, "Photonic-bandgap materials for high gain printed circuit antennas," *IEEE Trans. Anetennas Propagat.*, vol. 45, pp. 185–187, Jan. 1997.
[6] P. M. Bell, J. B. Pendry, L. Martin Moreno, and A. J. Ward, "A program for calculating photonic band structures and transmission coefficients of complex structures," *Comput. Phys. Commun.*, vol. 85, pp. 307–322, 1995.
[7] J. B. Pendry, "Photonic band structures," *J. Mod. Opt.*, vol. 41, no. 2, pp. 209–229, 1994.
[8] W. Y. Leung, R. Biswas, S. Cheng, M. M. Sigalas, J. S. McCalmont, G. Tuttle, and K. M. Ho, "Slot antennas on photonic band gap crystals," *IEEE Trans. Antennas Propagat.*, vol. 45, pp. 1569–1570, Oct. 1997.
[9] M. M. Sigalas, R. Biswas, K. M. Ho, W. Leung, G. Tuttle, and D. D. Crouch, "The effect of photonic crystals on dipole antennas," *Electromagnetics*, vol. 19, pp. 291–303, 1999.
[10] A. L. Reynolds and J. M. Arnold, "Interleaving two-dimensional lattices to create three-dimensional photonic band gap structures," *Proc. Inst. Elect. Eng.*, pt. J, vol. 145, pp. 436–440, Dec. 1998.
[11] H. S. Sozuer and J. P. Dowling, "Photonic band calculations for woodpile structures," *J. Mod. Opt.*, vol. 41, no. 2, pp. 231–239, 1994.
[12] E. Ozbay, E. Michel, G. Tuttle, R. Biswas, M. Sigalas, and K.-M. Ho, "Micro-machined millimeter wave photonic band gap crystals," *Appl. Phys. Lett.*, vol. 64, no. 16, pp. 2059–2061, 1994.
[13] E. Ozbay, B. Temelkuran, M. Sigalas, G. Tuttle, C. M. Soukoulis, and K. M. Ho, "Defect structures in metallic photonic crystals," *Appl. Phys. Lett.*, vol. 69, no. 25, pp. 3797–3799, 1996.
[14] E. Ozbay, E. Michel, G. Tuttle, R. Biswas, K.-M. Ho, J. Bostak, and D. M. Bloom, "Terahertz spectroscopy of three-dimensional photonic band-gap crystals," *Opt. Lett.*, vol. 19, no. 15, pp. 1155–1157, 1994.
[15] S. Y. Lin, J. G. Flemming, D. L. Hetherington, B. K. Smith, R. Biswas, K. M. Ho, M. M. Sigalas, W. Zubrzycki, S. R. Kurtx, and J. Bur, "A three-dimensional photonic crystal operating at infrared wavelengths," *Nature*, vol. 394, pp. 251–253, 1998.
[16] R. E. Collin, *Field Theory of Guided Waves*, 2nd ed. New York: IEEE Press, 1991.
[17] C. M. Anderson and K. P. Giapis, "Symmetry reduction in group 4 mm photonic crystals," *Phys. Rev. B, Condens. Matter*, vol. 54, no. 12, p. 7313, 1997.

Andrew L. Reynolds was born in Birmingham, U.K., in 1974. He received the European Master of Electronics Optoelectronics degree, and the M.Eng. (*cum laude*) and Ph.D. degrees from the University of Glasgow, Glasgow, Scotland, in 1996 and 2000, respectively.

In 1997, he spent one year as a Young Graduate Trainee in the Antenna Section, European Space Research and Technology Centre (ESTEC), Noordwijk, The Netherlands. He is currently with Nortel Networks UK Ltd., Harlow, Essex, U.K. His research interests are focused on photonic-bandgap materials to antenna and optoelectronic applications.

Harold M. H. Chong received the B.Eng. (with honors) degree in electronics and electrical engineering from the University of Glasgow, Glasgow, Scotland, in 1997, and is currently working toward the M.Sc. degree at the University of Glasgow.

From 1997 to 1998, he was a Telecommunications Engineer in the Department of Telecommunications, Ministry of Communications, Brunei Darussalam, Borneo. His research interests are millimeter-wave periodic structures, passive monolithic-microwave integrated-circuit (MMIC) devices, planar antennas, and micromachining substrates for RF applications.

Mr. Chong is a student member of the Institution of Electrical Engineers (IEE), U.K.

Iain G. Thayne, photograph and biography not available at time of publication.

John M. Arnold, photograph and biography not available at time of publication.

Peter de Maagt (S'88–M'88) was born in Pauluspolder, The Netherlands, in 1964. He received the M.Sc. and Ph.D. degrees from the Eindhoven University of Technology, Eindhoven, The Netherlands, in 1988 and 1992, respectively, both in electrical engineering.

He is currently with the European Space Research and Technology Centre (ESTEC), European Space Agency, Noordwijk, The Netherlands. His research interests are in the area of millimeter and submillimeter-wave reflector and planar integrated antennas, quasi-optics, PBG antennas, and millimeter- and sub-millimeter-wave components.